MODEL-BASED SIGNAL PROCESSING TECHNIQUES FOR ULTRASONIC FLAW DETECTION: SIMULATION STUDIES

Chien-Ping Chiou[1], R. Bruce Thompson[2] and Lester W. Schmerr[2]
[1]Center for Aviation Systems Reliability and
[2]Center for NDE and
Department of Aerospace Engineering and Engineering Mechanics
Iowa State University
Ames, Iowa 50011

INTRODUCTION

The ultrasonic signals observed in inspection processes can often be accurately predicted by suitable measurement models. These model predictions can be used to provide important information to guide the development of subsequent signal processing algorithms. Here such a hybrid use of ultrasonic modeling and signal processing is demonstrated in the context of the problem of detecting ultrasonic flaw signals in noise. In particular, we wish to apply this hybrid methodology as an initial approach to solving the problem of detecting hard-alpha inclusions in titanium alloys.

The "hard-alpha" inclusions are known to be brittle regions of microstructure caused by oxygen or nitrogen contaminations. During high-stressed manufacturing process or in-service operations, they are likely to initiate cracking, which may subsequently leads to catastrophic failure of aircraft components [1]. Hence, early detection is desired. However, the inherently weak strength of signals from hard-alpha inclusions, complicated further by the presence of high-level correlated grain noise, have long rendered this a particularly serious inspection problem. Furthermore, the lack of appropriate test specimens has made the development and evaluation of detection techniques even more challenging.

In our engineering approach toward this problem, we first utilize a measurement model to simulate signals for specific inclusions and superimpose on these noise traces obtained on real samples. We then show that it is feasible to construct matched filters to achieve significant signal-to-noise ratio (SNR) enhancement. Based on simulation studies of large-scale data sets, we can then assess the matched filter performance and the detectability in terms of the receiver operating characteristics estimates. Examples of detection of different inclusion impedances and sizes are presented in combination with various experimental setups. The results of using split-spectrum technique are also included. A parallel effort of applying neural networks and statistical analysis to the hard-alpha problem can be found in these proceedings [2].

SIGNAL SIMULATION

The manufacture of test specimens containing seeded hard-alpha inclusions is currently underway in a separate work [3]. Presently, it is believed that these hard-alpha inclusions have similar ultrasonic characteristics as those of weakly scattering inclusions, and can be simulated from models [4]. Here the Thompson-Gray measurement model [5] is employed to simulate the hard-alpha inclusion signals. This model simulates flaw signals through modeling of the entire ultrasound propagation process using theoretical calculations of flaw scattering amplitude, beam spreading, medium attenuation and interface transmission. The electronic system response is introduced through waveforms obtained from a separate reference experiment. At given range of depth in a titanium specimen, the flaw time record can be synthesized by adding real grain noise data to the simulated flaw signals. Although the software is capable of simulating ellipsoidal flaw signals using both planar and focused probes on flat or curved interface, our current studies are limited to a spherical inclusion and flat interface only for simplicity. Using this additive data model, we have acquired two large-scale data sets of different flaw and transducer specifications for testing our signal processing algorithms. The characteristics of the two data sets are summarized in Table 1 as data sets 1 and 3. The specimen is a typical Ti-6426 alloy block having a moderately severe noise. It is seen that, with the use of focused transducer, the average input SNR in Set 3 is better than that of Set 1 although the inclusion size in Set 3 is less than half as large as in Set 1. Set 3 also has a smaller contrast in acoustic impedance of 10% higher than the host titanium alloy. The peak SNR here is defined by the division of the peak inclusion signal by the peak noise signal in a noise trace.

The other signal (data) simulation method applied in this work is a recent Monte-Carlo noise model [6]. Utilizing the Thompson-Gray model as the building block, this model computes the ultrasonic scattering contributions from individual grains as well as the target flaw. The flaw data are then the superposition of total responses from flaw and grains within the beam boundary. This noise model has also confirmed the validity of the first additive model by producing flaw data of the same characteristics. Data set 2 in Table 1 lists one set of flaw data generated from noise model.

The simulated data from both models have been analyzed to be approximately Gaussian distributed with zero mean (after DC component removal) outside the flaw region (i.e. the grain noise portion). This Gaussian behavior is more closely reproduced for the planar probe data which contain longer time records. Within the flaw region, the mean is influenced by the flaw signal and depends on the flaw signal strength. From further analysis, the grain noise was considered colored mainly by the transducer spectrum. It was also determined that, for short-time data, non-stationarity due to material attenuation is small and can be ignored. However, this is not the case for the non-stationarity caused by the transducer focusing effect.

MATCHED FILTER TECHNIQUE

In the signal simulation, as stated above, the expected form of the flaw signals are known which naturally lead us to the use of matched filter techniques. In matched filters, one matches the filter impulse response to the flaw signal so that the instantaneous peak correlation effect is maximized. This method was originally developed and widely used in the radar area [7] and has appeared in NDE applications [8]. The feasibility and advantages of applying this filter to the hard-alpha detection problem are four-fold. First, in principle it is the optimal linear filter for detecting known signals in colored noise. Secondly, the approach can be easily adjusted as knowledge of actual flaw signal waveforms become available later. The adjustment can be done through further modeling refinement or empirical signal acquisition. Thirdly, the flaw size can be simultaneously estimated in a M-ary system of multiple matched filter banks. Fourthly, in order to avoid solving complicated integral equations in its full implementation, a simpler frequency domain approximation can be employed taking advantage of assumed past and future behavior of the signal. This approximation is computationally efficient via the Fast Fourier Transform algorithm and is capable of real-time inspections. The frequency response of the approximated filter takes the form [9]:

$$H(f) \propto \frac{F^*(f)}{S(f)} \tag{1}$$

Where $F^*(f)$ is the conjugate of flaw frequency response and $S(f)$ is the noise power spectrum. The division by $S(f)$ is to pre-whiten the noise spectrum since the generic matched filter was derived for white noise [9]. Here several algorithms were applied to estimate $S(f)$ including Welch's multi-windowing periodogram [10] and the simple use of

Table 1 The descriptions of three simulated data sets.

Description	Data Set 1	Data Set 2	Data Set 3
data set size	100	42	231
inclusion signal	simulated	simulated	simulated
noise signal	real	simulated	real
inclusion diameter in μm	1000	400	400
inclusion impedance difference	high	medium	low
average input signal-to-noise ratio	-3.78	1.6	-2
transducer bandwidth in MHz	(0.6, 23)	(3.0,6.9)	(0.4,12.0)
transducer type	planar 0.25" dia	focused 0.5", F = 2"	focused 0.5", F = 2"

spectrum magnitude. We found that, practically, the simple spectrum magnitude gave best results in spite of the fact that it is theoretically an inconsistent estimator. We computed the noise power spectrum estimate using the same noise data before superimposing it on the flaw signal. In practice, additional techniques will be required to estimate S(f) from waveforms which might contain flaw signals.

Three versions of the matched filter, namely, white, gated-color and color, were developed for evaluation. The white version contains the basic form of F*(f) without the S(f) whitening component in (1). The gated-color filter is the time-limited finite impulse response (FIR) version having duration about the same as the flaw signal, and the color version implements the band-limited infinite impulse response (IIR) circular correlation. All three filter versions have been tested on data set 1 (Table 1) and their performance comparison is listed in Fig. 1. The color version is seen superior to other two in enhancing peak SNR. With input average peak SNR of -3.78 dB, the color filter is able to obtain significant average peak SNR enhancement of more than 11 dB at the output. This color version was then selected for subsequent testing of other data sets.

One detection example obtained from Set 3 data is illustrated in Figs. 2 (a)-(d). Fig. 2 (a) shows a 400 μm hard-alpha spherical inclusion signal simulated for a focused immersion setup. Because of its small size, the echoes from front and back specular points of this inclusion can not be resolved. When synthesized with a corresponding experimental rf noise data set, this inclusion signal is completely corrupted (at the location pointed by an upward arrow) which leads to a poor input peak SNR of -1.5 dB (Fig. 2 (b)). After a matched filter designed for a 400 μm flaw is applied, the flaw signal is greatly enhanced to indicate a sure detection (Fig. 2 (c)). In contrast, Fig. 2(d) depicts the filtered result of the corresponding noise data (in the absence of flaw signal) with much lower level of enhancement, which gives an output peak SNR of 9.1 dB and a peak SNR enhancement of 10.6 dB. The time resolution of detection is also exceptional. By aligning the time axes of Figs. 2(a) and 2(c), we can see that the filtered signal peaks up right at the center of the flaw signal before filtering, which is as expected from the preset filter delay.

As shown in Fig. 2, the result of using the filter of matched size has implied the actual implementation of a M-ary system. The M-ary system involves sending the same input signal to a series of filter banks where each filter bank is targeting for a specific flaw size so that maximum matching to the input signal, and hence the detection, can be ensured. In this way, we gain the extra advantage of being able to estimate the flaw size simultaneously. Fig. 3 demonstrates this concept of using an M-ary system where five data records, each

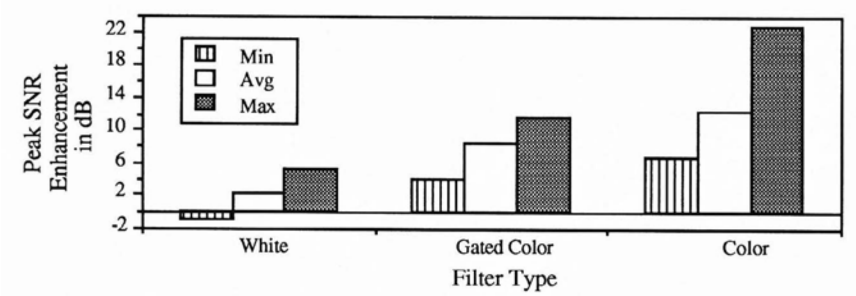

Fig. 1 The performance comparison of three versions of a matched filter. Min, Avg and Max refer to the performance on the 100 waveforms in data set 1.

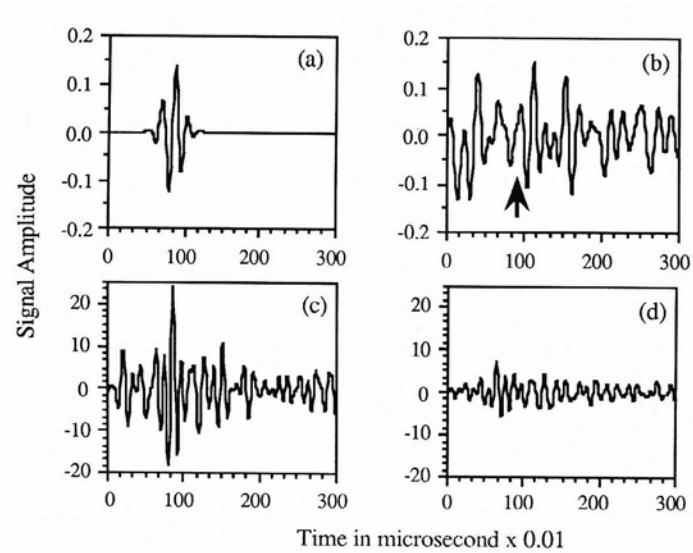

Fig. 2 A simulated low-impedance 400 μm hard-alpha inclusion signal (a), the superimposition of (a) on an experimental grain noise measurement (b), the result of (b) after matched filtering (c), and the filtered result of noise only (d).

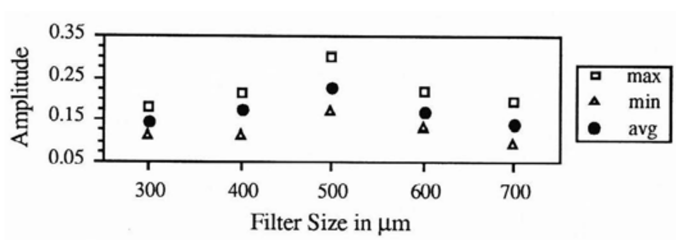

Fig. 3 The amplitude distributions of a M-ary matched filter system with respect to five input noise data waveforms, each containing a 500 μm inclusion signal.

containing a 500 μm flaw signal, were processed through 5 filters matched to different flaw size ranging from 300 μm to 700 μm. It is evident that the 500 μm filter indeed outperforms the others in obtaining the highest filtered amplitude. It is also observed from Fig. 3 that the filtered amplitudes of other filters do not decline abruptly. This mismatch insensitivity would be beneficial for detection in that the neighboring filters may still be able to detect a distorted input signal if the filter of exact match has failed to do so. It also suggest that the technique may be robust to variations in flaw shape from the assumed sphere.

The receiver operating characteristics of the matched filter was examined by employing statistical hypothesis testing [9]. One likelihood-ratio test, the Neyman-Pearson criterion, was considered suitable for our problem, since it requires neither a priori probabilities nor cost estimates which are difficult to determine in practice. Derived from the general Bayes criterion as a special case, the Neyman-Pearson criterion maximizes the probability of detection (POD) for a given probability of false alarm (POF). Here POD and POF for detecting signals in Gaussian noise can be related implicitly through the following expressions

$$\mathrm{POF} = \frac{1}{2}\,\mathrm{erfc}\,(x) \tag{2}$$

and

$$\mathrm{POD} = \frac{1}{2}\,\mathrm{erfc}\left(x - \sqrt{\frac{P}{2}}\right) \tag{3}$$

where P is the output power peak signal to RMS noise ratio and erfc(x) is the complementary error function defined by

$$\mathrm{erfc}(x) \equiv \sqrt{\frac{2}{\pi}} \int_x^\infty \exp(-t^2)\, dt \tag{4}$$

Fig. 4 plots the performance comparison of these Neyman-Pearson POD-POF predictions vs. the simulation results using the three data sets in Table 1. The theoretical POD's were computed, for given POF's and P's, from (3) by first solving for the dimensionless variable x in (2) iteratively. The POD's and POF's in the simulation results were obtained by properly thresholding the output signals processed by the matched filters. The Set 1 data points (with output power SNR of 8) distribute precisely in-between the two theoretical curves of power SNR's of 6 and 10. The Set 3 data points, having the highest output SNR of 20, follow the similar trend initially but, owing to the presence of a few outliers, level off earlier than the projected theoretical prediction. Set 2 data, having few available data points, deviate considerably more from the ideal predictions. Nevertheless, overall good agreement between the theory and the simulation is observed. At the 10% POF level, at least 92% POD has been reached in all three data sets.

SPLIT-SPECTRUM TECHNIQUE

Another technique known as split-spectrum (frequency diversity) has also been implemented in this work. This method, appearing in the field for nearly a decade ago [11], is capable of suppressing grain noise through a number of bandpass filterings that decrease the correlation between signal components. The flaw detection task is then accomplished by post-processing each of these filtered signals back in time domain using some non-linear algorithms including minimization and polarity thresholding [12]. These algorithms mostly rely on the relative stability of flaw signal amplitude and polarity over the noise counterparts in the decorrelation process. For strong scatterers (such as flat-bottom holes), which possess higher reflectivity and a characteristic spectrum that is distinct from that of grain boundaries, this method has been shown to work well [12]. For our problem where inclusion signals are generally weaker with overlapping spectrum, however, certain modifications are necessary. In conjunction with the use of additional lowpass filtering and polarity change tolerance, the hybrid minimization/polarity thresholding algorithm using sinusoidal windows [13] was the best choice for most situations.

Fig. 5 illustrates one detection example of a simulated 1000 μm high-impedance hard-alpha inclusion signal obtained from a 10MHz planar immersion scan. Fig. 5 (a) shows the superposition of the inclusion signal and high grain noise background which gives a poor peak input SNR of about -6 dB. The split-spectrum processing was performed in the spectral range of 1.1 - 4 MHz (equivalent to a low pass filtering), with window center frequency separation of 0.2 MHz, window width of 0.3 MHz, and cosine taper of 0.2 MHz. The tolerance for polarity change was set to 5. The filtered output, as shown in Fig. 5 (b), peaks up highest in the flaw region but also retains other structure in the early time, which leads to a moderate output peak SNR of 2.5 dB and an SNR enhancement of 8.5 dB. From testing other cases, we found that, with all the previously mentioned modifications, the split spectrum algorithm can reach the SNR enhancement comparable to that obtained from the matched filter. However, as previously reported in the literature, this technique is also found very sensitive to the parameter settings which are usually difficult to obtain a priori in practice.

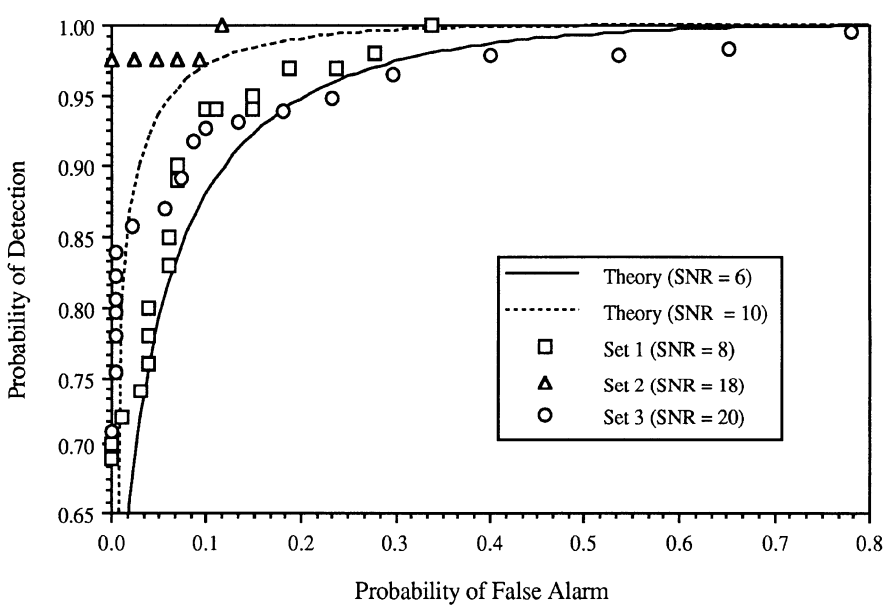

Fig. 4 Operating characteristics of Neyman-Pearson theory vs. three data set simulations.

SUMMARY AND DISCUSSION

In this work, we have demonstrated the feasibility of using signal modeling/processing techniques to detect interior volumetric flaw (particularly hard-alpha inclusions) signals corrupted by material noise. POD above 90% and POF below 10% are also shown achievable through large-scale testing for the particular simulated inclusion signals studied. Both the matched filter and split spectrum methods have comparable performance but the matched filter is more consistent.

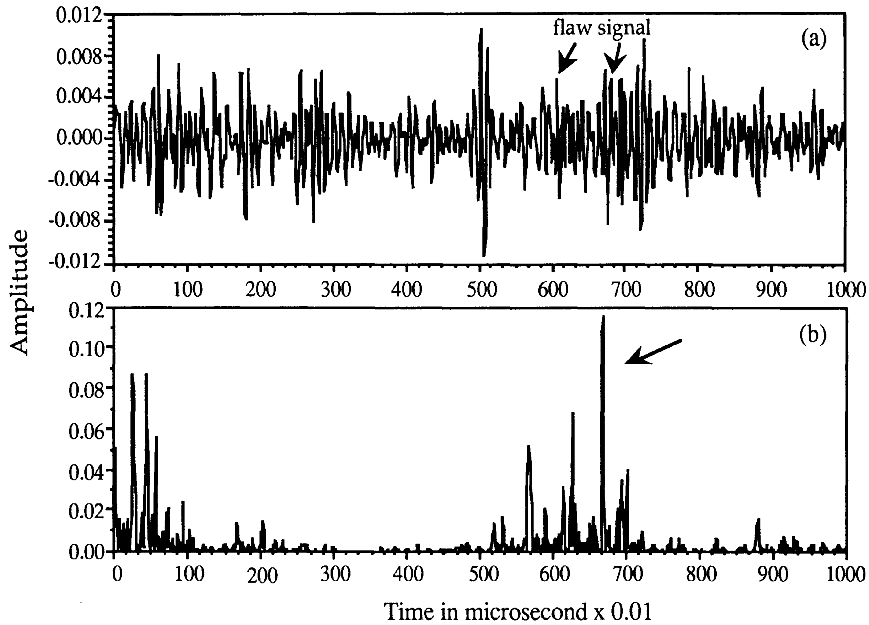

Fig. 5 Detection example of hard-alpha inclusion using split-spectrum technique: a weak inclusion signal surrounded by severe grain noise (a) and the filtered result (b).

ACKNOWLEDGEMENTS

The authors would like to thank Drs. Isaac Yalda-Mooshabad and Frank J. Margetan for providing us their simulated ultrasonic data. Thanks are also due to Mr. Bob Forouraghi for his comments on the manuscript and to Ms. Lisa Brasche for her general assistance. This work was sponsored by the FAA-Center for Aviation Systems Reliability, operated by the Ames Laboratory, USDOE, for the Federal Aviation Administration under contract No. W-7405-ENG-82 with Iowa state University. This work was also supported by the NSF Industry/University Center for NDE at Iowa State University.

REFERENCES

1. J. G. Costa, R. E. Gonzalez, R. E. Guyotte, D. P. Salvano, T. Swift and R. J. Koenig, Titanium Rotating Components Review Team Report, Federal Aviation Administration, Washington, December 1990.

2. C.-P. Chiou, L. W. Schmerr and R. B. Thompson, "Ultrasonic Flaw Detection Using Neural Network Models and Statistical Analysis: Simulation Studies," these proceedings.

3. L. J. H. Brasche, F. J. Margetan and R. B. Thompson, "Sample Preparation Techniques and Material Property Measurements of Hard Alpha Titanium Samples," Review of Progress in Quantitative Nondestructive Evaluation Vol 11B, (Eds. D. O. Thompson and D. E. Chimenti) Plenum Press, New York, pp. 1733-1738, 1992.

4. F. J. Margetan and R. B. Thompson, "Microstructural Noise in Titanium Alloys and Its Influence on the Detectability of Hard-Alpha Inclusions," Review of Progress in Quantitative Nondestructive Evaluation Vol 11B, (Eds. D. O. Thompson and D. E. Chimenti) Plenum Press, New York, pp. 1717-1724, 1992.

5. R. Bruce Thompson and Tim Gray, "A Model Relating Ultrasonic Scattering Measurements Through Liquid-Solid Interfaces to Unbounded Medium Scattering Amplitudes," Journal of Acoustical Society of America, 74, pp. 1279-1290, 1983.

6. I. Yalda-Mooshabad, F. J. Margetan and R. B. Thompson, "Monte-Carlo Simulation of Ultrasonic Grain Noise," these proceedings.

7. D. O. North, Analysis of Factors Which Determine Signal-to-Noise Discrimination in Radar, RCA Laboratories, Princeton, New Jersey, Rept. PTR-6c, June 1943.

8. J.-Q. Xin, K. D. Donohue and N. M. Bilgutay, "Filter Design for Ultrasonic Flaw Echo Detection in Large-Grained Material," Review of Progress in Quantitative Nondestructive Evaluation Vol 10A, (Eds. D. O. Thompson and D. E. Chimenti) Plenum Press, New York, pp. 725-731, 1991.

9. H. L. Van Trees, Detection, Estimation, and Modulation Theory, Part I, John Wiley and Sons, Inc., New York, 1968.

10. S. L. Marple, Jr., Digital Spectral Analysis with Applications, Prentice-Hall, New Jersey, 1987.

11. V. L. Newhouse, N. M. Bilgutay, J. Saniie and E. S. Furgason, "Flaw-to-Grain Echo Enhancement by Split-Spectrum Processing," Ultrasonics, 20, 2, pp. 59-68, 1982.

12. L. Yue and Y. Chong-Fu, "Two Signal Processing Techniques for the Enhancement of the Flaw-to-Grain Echo Ratio," Ultrasonics, 25, 3, pp. 90-94, 1987.

13. O. J. Canelones and P. Karpur, "Split-Spectrum Processing with Computationally Efficient Sinusoidal FIR Filters," Review of Progress in Quantitative Nondestructive Evaluation Vol 11A, (Eds. D. O. Thompson and D. E. Chimenti) Plenum Press, New York, pp. 935-942, 1992.